SUPPLEMENTARY FIGURES

Number of Supplemental Figures: 12.

Number of Supplemental Tables: 2.

Fig.S1

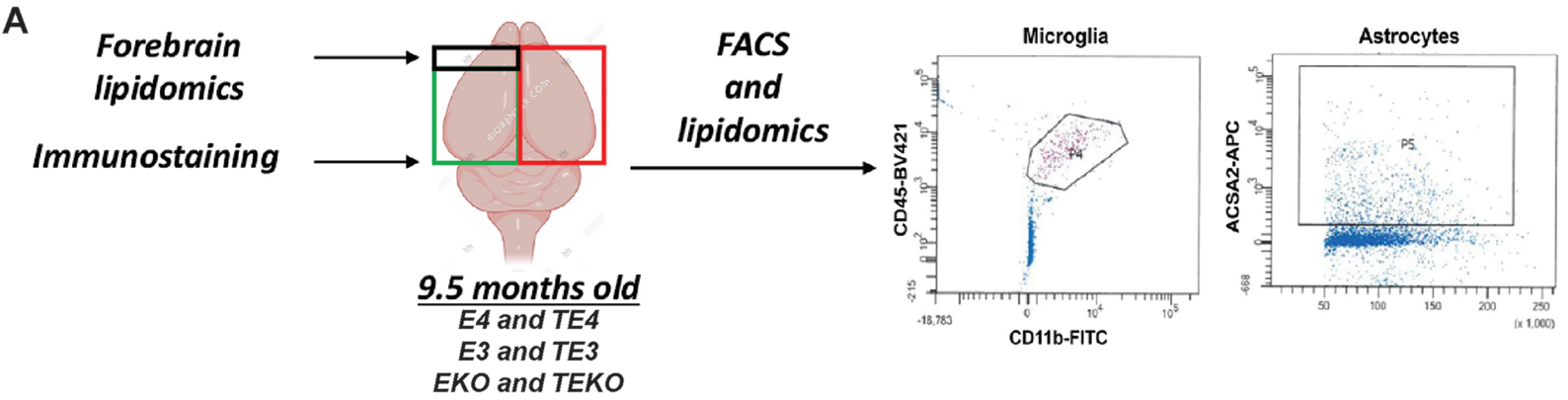
A
Forebrain lipidomics
Immunostaining
FACS and lipidomics
Microglia
Astrocytes
CD45-BV421
CD11b-FITC
ACSA2-APC
9.5 months old
E4 and TE4
E3 and TE3
EKO and TEKO

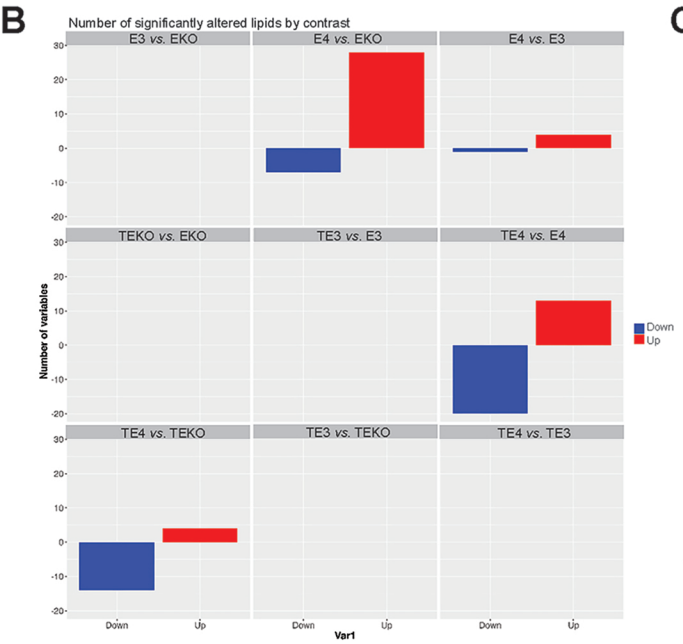
B
Number of significantly altered lipids by contrast
E3 vs. EKO
E4 vs. EKO
E4 vs. E3
TEKO vs. EKO
TE3 vs. E3
TE4 vs. E4
TE4 vs. TEKO
TE3 vs. TEKO
TE4 vs. TE3
Number of variables
Down
Up
Var1

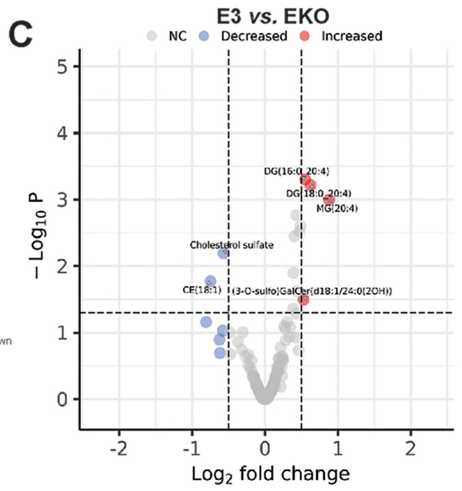
C
E3 vs. EKO
NC
Decreased
Increased
DG(16:0_20:4)
DG(18:0_20:4)
MG(20:4)
Cholesterol sulfate
CE(18:1)
(3-O-sulfo)GalCer(d18:1/24:0(2OH))
Log2 fold change

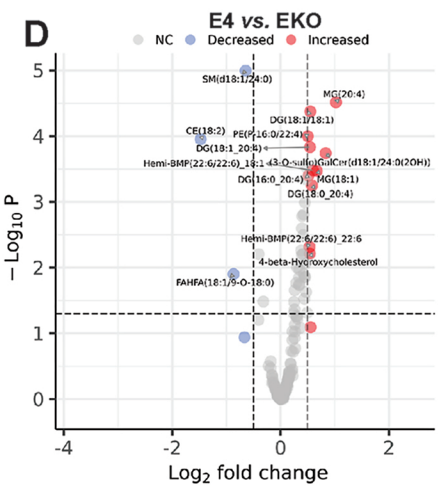
D
E4 vs. EKO
NC
Decreased
Increased
SM(d18:1/24:0)
MG(20:4)
DG(18:1/18:1)
CE(18:2)
DG(18:1_20:4)
Hemi-BMP(22:6/22:6)_18:1
DG(16:0_20:4)
MG(18:1)
DG(18:0_20:4)
Hemi-BMP(22:6/22:6)_22:6
4-beta-Hydroxycholesterol
FAHFA(18:1/9-O-18:0)
Log2 fold change

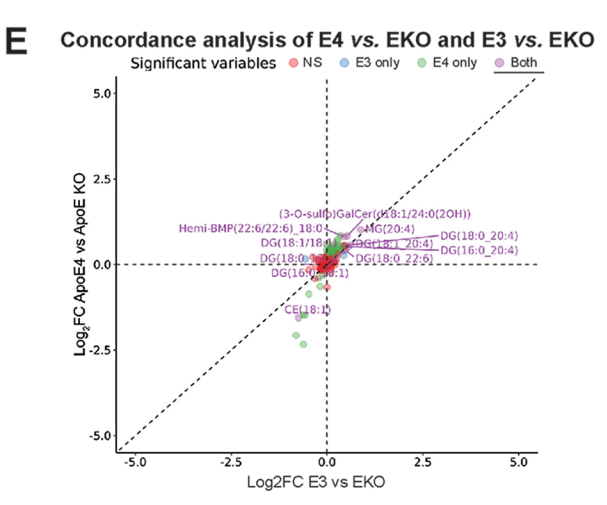
E
Concordance analysis of E4 vs. EKO and E3 vs. EKO
Significant variables
NS
E3 only
E4 only
Both
(3-O-sulfo)GalCer(d18:1/24:0(2OH))
Hemi-BMP(22:6/22:6)_18:0
MG(20:4)
DG(18:1/18:1)
DG(18:1_20:4)
DG(18:0_20:4)
DG(16:0_20:4)
DG(18:0_22:6)
DG(16:0_20:1)
CE(18:1)
Log2FC ApoE4 vs ApoE KO
Log2FC E3 vs EKO

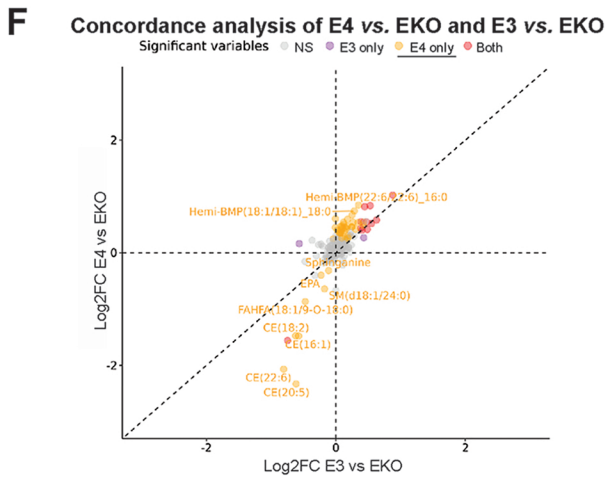
F
Concordance analysis of E4 vs. EKO and E3 vs. EKO
Significant variables
NS
E3 only
E4 only
Both
Hemi-BMP(22:6/22:6)_16:0
Hemi-BMP(18:1/18:1)_18:0
Spermine
EPA
SM(d18:1/24:0)
FAHFA(18:1/9-O-18:0)
CE(18:2)
CE(16:1)
CE(22:6)
CE(20:5)
Log2FC E4 vs EKO
Log2FC E3 vs EKO

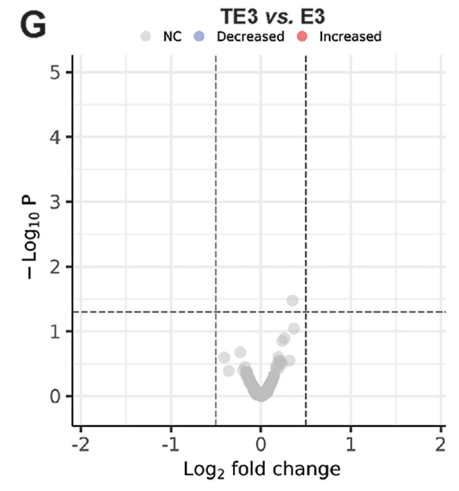
G
TE3 vs. E3
NC
Decreased
Increased
Log2 fold change

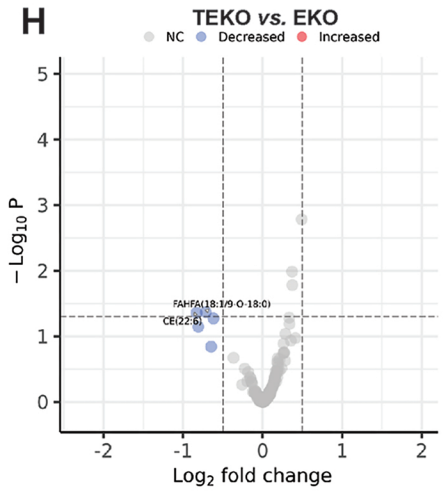
H
TEKO vs. EKO
NC
Decreased
Increased
FAHFA(18:1/9-O-18:0)
CE(22:6)
Log2 fold change

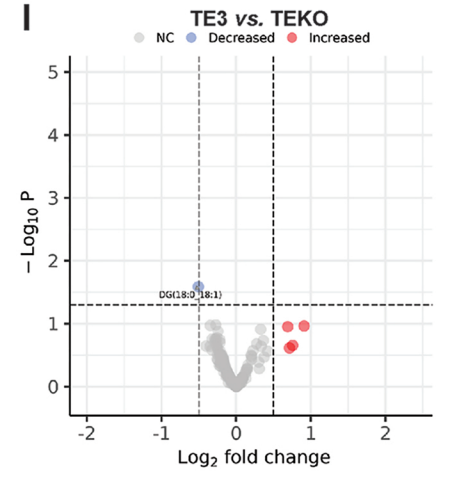
I
TE3 vs. TEKO
NC
Decreased
Increased
DG(18:0_18:1)
Log2 fold change

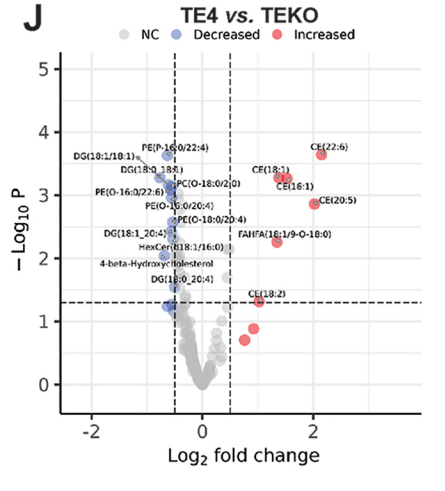
J
TE4 vs. TEKO
NC
Decreased
Increased
PE(P-16:0/22:4)
DG(18:1/18:1)
DG(18:0_18:1)
PC(O-18:0/2:0)
PE(O-16:0/22:6)
PE(O-16:0/20:4)
PE(O-18:0/20:4)
DG(18:1_20:4)
HexCer(d18:1/16:0)
4-beta-Hydroxycholesterol
DG(18:0_20:4)
CE(22:6)
CE(18:1)
CE(16:1)
CE(20:5)
FAHFA(18:1/9-O-18:0)
CE(18:2)
Log2 fold change

Fig.S2

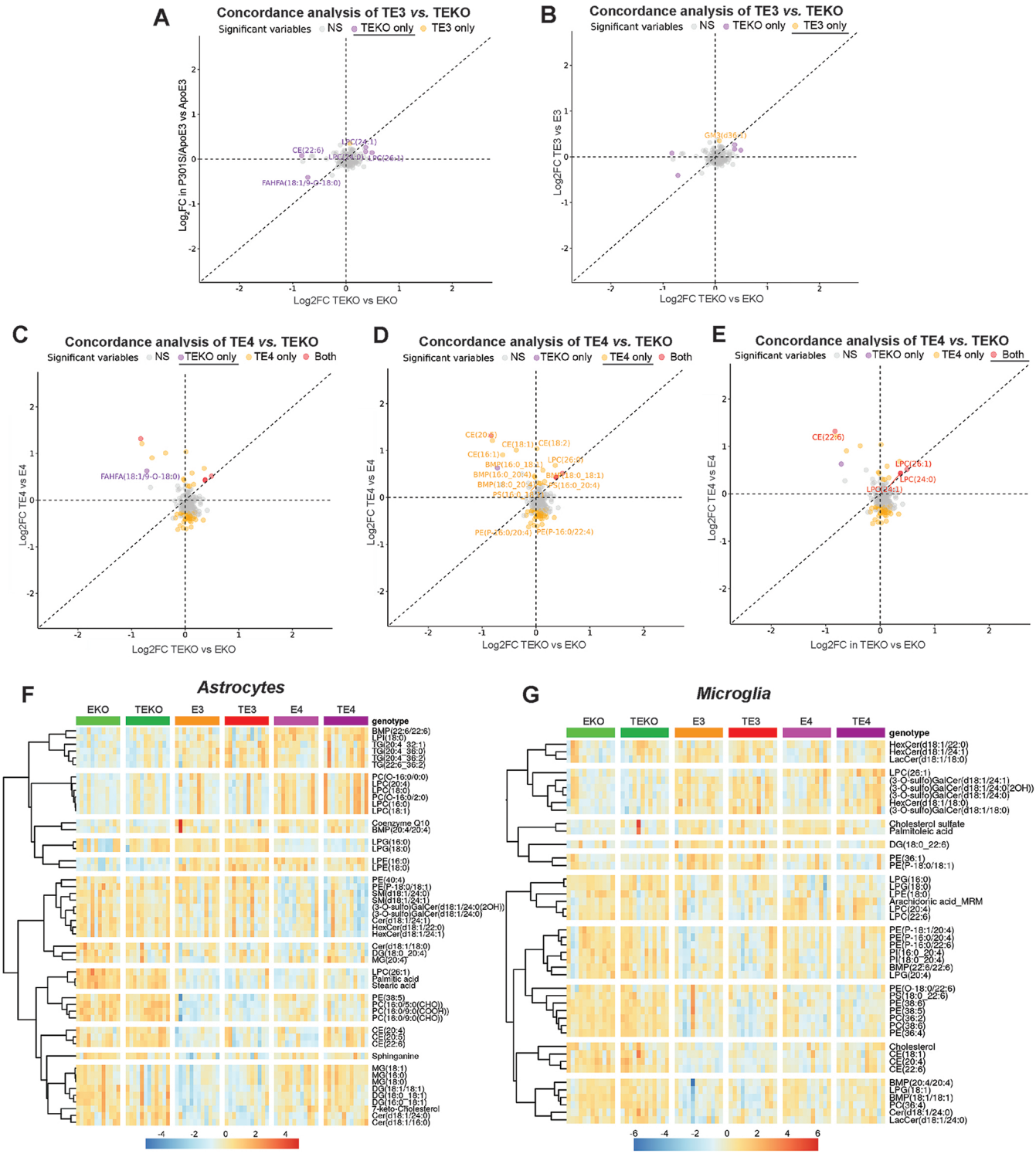
A
Concordance analysis of TE3 vs. TEKO
Significant variables NS TEKO only TE3 only
Log2FC in P301S/ApoE3 vs ApoE3
Log2FC TEKO vs EKO
CE(22:6)
LPC(24:1)
LPC(24:0)
LPC(26:1)
FAHFA(18:1/9-O-18:0)
B
Concordance analysis of TE3 vs. TEKO
Significant variables NS TEKO only TE3 only
Log2FC TE3 vs E3
Log2FC TEKO vs EKO
GM3(d36:1)
C
Concordance analysis of TE4 vs. TEKO
Significant variables NS TEKO only TE4 only Both
Log2FC TE4 vs E4
Log2FC TEKO vs EKO
FAHFA(18:1/9-O-18:0)
D
Concordance analysis of TE4 vs. TEKO
Significant variables NS TEKO only TE4 only Both
Log2FC TE4 vs E4
Log2FC TEKO vs EKO
CE(20:5)
CE(18:1)
CE(18:2)
CE(16:1)
LPC(26:0)
BMP(16:0_18:1)
BMP(16:0_20:4)
BMP(18:1_18:1)
BMP(18:0_20:4)
PS(16:0_20:4)
PE(P-16:0/20:4)
PE(P-16:0/22:4)
E
Concordance analysis of TE4 vs. TEKO
Significant variables NS TEKO only TE4 only Both
Log2FC TE4 vs E4
Log2FC in TEKO vs EKO
CE(22:6)
LPC(26:1)
LPC(24:0)
LPC(24:1)
F
Astrocytes
EKO TEKO E3 TE3 E4 TE4
genotype
BMP(22:6/22:6)
LPI(18:0)
TG(20:4_32:1)
TG(20:4_36:0)
TG(20:4_36:2)
TG(22:6_36:2)
PC(O-16:0/0:0)
LPC(20:4)
LPC(16:0)
PC(O-16:0/2:0)
LPC(18:1)
Coenzyme Q10
BMP(20:4/20:4)
LPG(16:0)
LPG(18:0)
LPE(16:0)
LPE(18:0)
PE(40:4)
PE(P-18:0/18:1)
SM(d18:1/24:0)
SM(d18:1/24:1)
(3-O-sulfo)GalCer(d18:1/24:0(2OH))
(3-O-sulfo)GalCer(d18:1/24:0)
Cer(d18:1/24:1)
HexCer(d18:1/22:0)
HexCer(d18:1/24:1)
Cer(d18:1/18:0)
DG(18:0_20:4)
MG(20:4)
LPC(26:1)
Palmitic acid
Stearic acid
PE(38:5)
PC(16:0/5:0(CHO))
PC(18:0/9:0(COOH))
PC(16:0/9:0(CHO))
CE(20:4)
CE(20:5)
CE(22:6)
Sphinganine
MG(18:1)
MG(18:0)
MG(18:0)
DG(18:1/18:1)
DG(18:0_18:1)
DG(16:0_18:1)
7-keto-Cholesterol
Cer(d18:1/24:0)
Cer(d18:1/16:0)
-4 -2 0 2 4
G
Microglia
EKO TEKO E3 TE3 E4 TE4
genotype
HexCer(d18:1/22:0)
HexCer(d18:1/24:1)
LacCer(d18:1/18:0)
LPC(26:1)
(3-O-sulfo)GalCer(d18:1/24:1)
(3-O-sulfo)GalCer(d18:1/24:0(2OH))
(3-O-sulfo)GalCer(d18:1/24:0)
HexCer(d18:1/18:0)
(3-O-sulfo)GalCer(d18:1/18:0)
Cholesterol sulfate
Palmitoleic acid
DG(18:0_22:6)
PE(36:1)
PE(P-18:0/18:1)
LPG(16:0)
LPG(18:0)
LPE(18:0)
Arachidonic acid_MRM
LPC(20:4)
LPC(22:6)
PE(P-18:1/20:4)
PE(P-16:0/20:4)
PE(P-16:0/22:6)
PI(16:0_20:4)
PI(18:0_20:4)
BMP(22:6/22:6)
LPG(20:4)
PE(O-18:0/22:6)
PS(18:0_22:6)
PE(38:6)
PE(38:5)
PC(36:2)
PC(38:6)
PE(36:4)
Cholesterol
CE(18:1)
CE(20:4)
CE(22:6)
BMP(20:4/20:4)
LPG(18:1)
PC(18:1/18:1)
PC(36:4)
Cer(d18:1/24:0)
LacCer(d18:1/24:0)
-6 -4 -2 0 2 4 6

Fig.S3

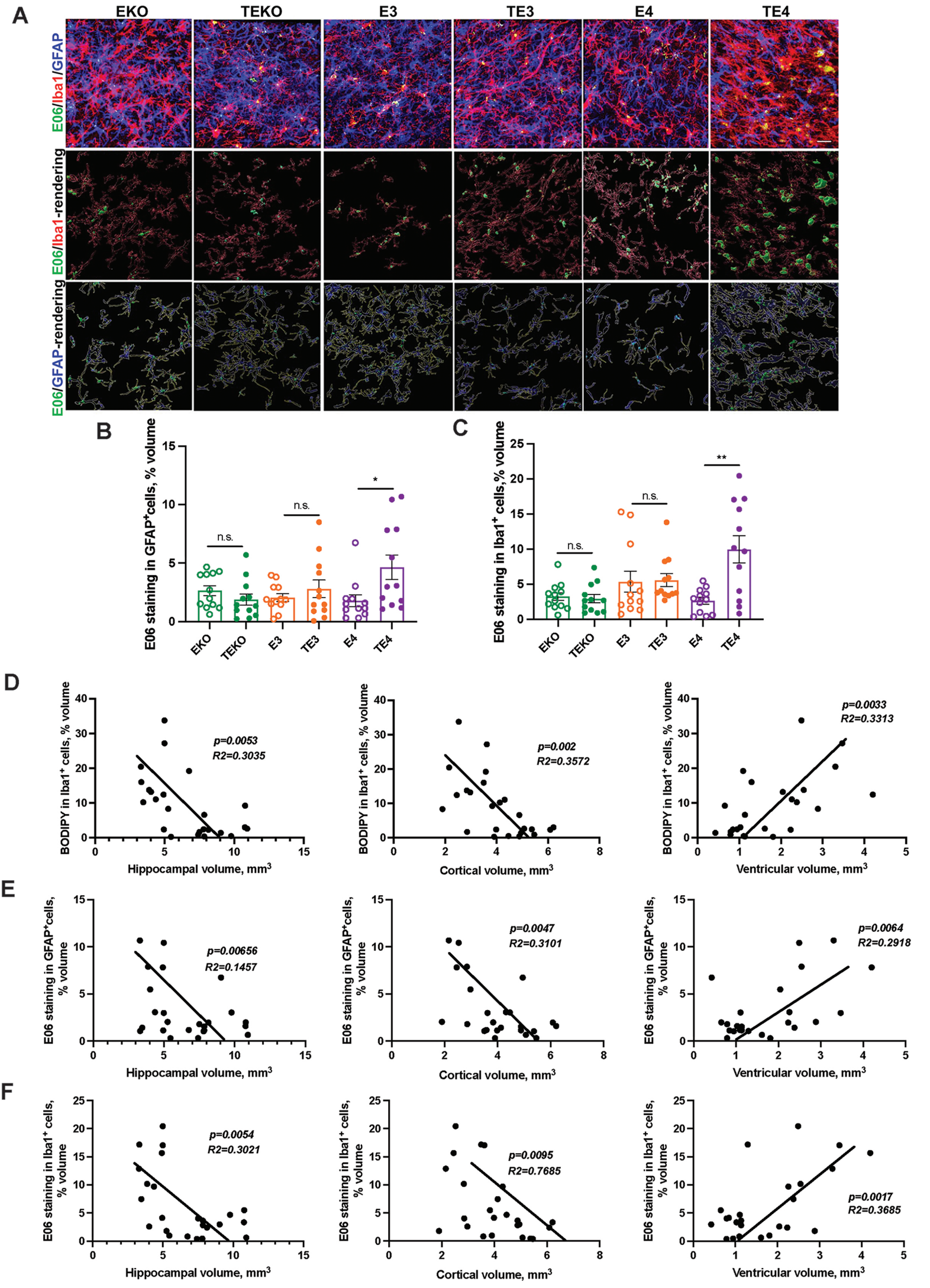
A
EKO
TEKO
E3
TE3
E4
TE4
E06/Iba1/GFAP
E06/Iba1-rendering
E06/GFAP-rendering
B
E06 staining in GFAP+cells, % volume
n.s.
n.s.
*
C
E06 staining in Iba1+ cells,% volume
n.s.
n.s.
**
D
BODIPY in Iba1+ cells, % volume
p=0.0053
R2=0.3035
Hippocampal volume, mm3
p=0.002
R2=0.3572
Cortical volume, mm3
p=0.0033
R2=0.3313
Ventricular volume, mm3
E
E06 staining in GFAP+cells, % volume
p=0.00656
R2=0.1457
Hippocampal volume, mm3
p=0.0047
R2=0.3101
Cortical volume, mm3
p=0.0064
R2=0.2918
Ventricular volume, mm3
F
E06 staining in Iba1+ cells, % volume
p=0.0054
R2=0.3021
Hippocampal volume, mm3
p=0.0095
R2=0.7685
Cortical volume, mm3
p=0.0017
R2=0.3685
Ventricular volume, mm3

Fig.S4

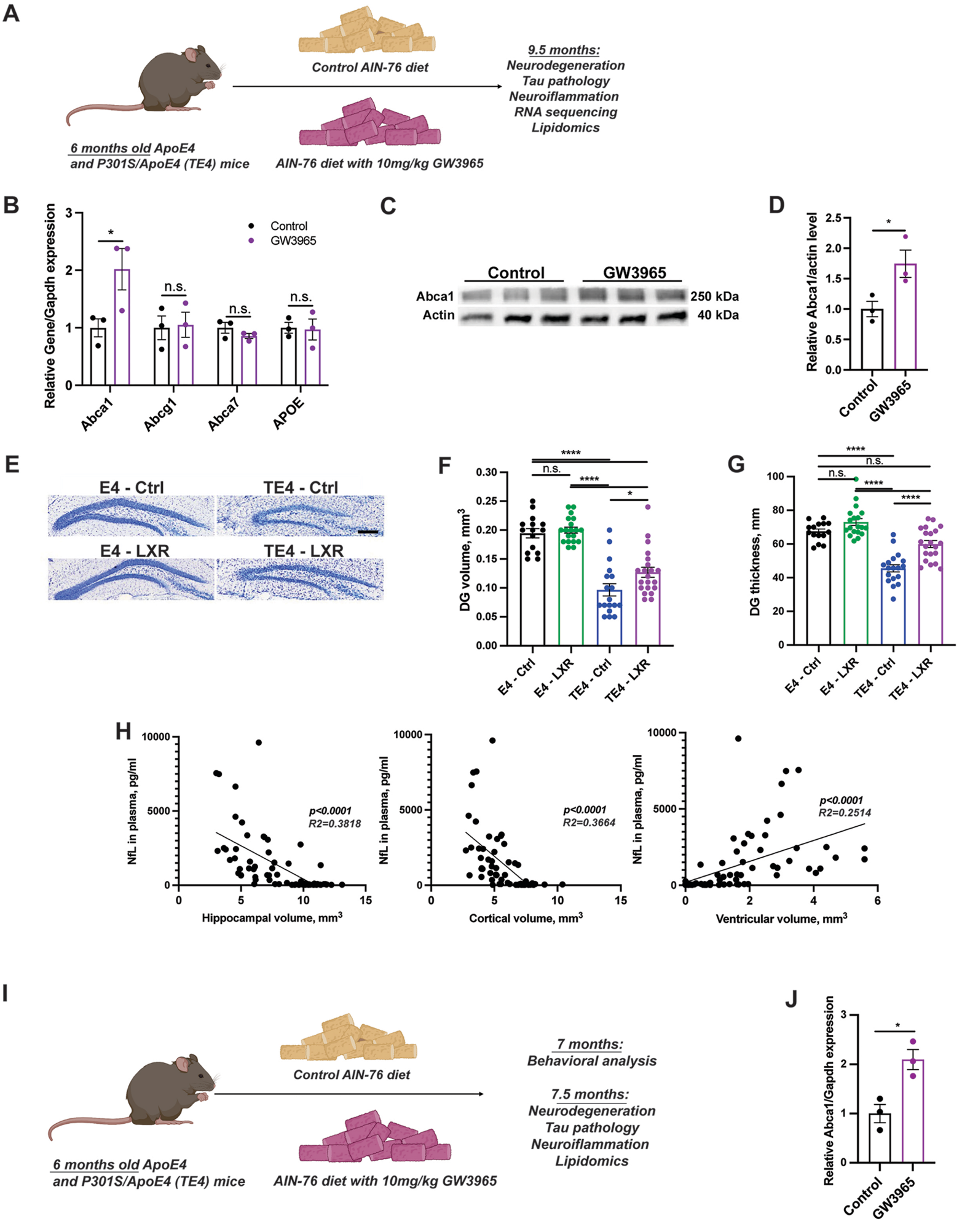
A
Control AIN-76 diet
9.5 months:
Neurodegeneration
Tau pathology
Neuroiflammation
RNA sequencing
Lipidomics
6 months old ApoE4
and P301S/ApoE4 (TE4) mice
AIN-76 diet with 10mg/kg GW3965
B
Relative Gene/Gapdh expression
Control
GW3965
*
n.s.
n.s.
n.s.
Abca1
Abcg1
Abca7
APOE
C
Control
GW3965
Abca1
Actin
250 kDa
40 kDa
D
Relative Abca1/actin level
*
Control
GW3965
E
E4 - Ctrl
TE4 - Ctrl
E4 - LXR
TE4 - LXR
F
DG volume, mm3
****
n.s.
****
*
E4 - Ctrl
E4 - LXR
TE4 - Ctrl
TE4 - LXR
G
DG thickness, mm
****
n.s.
n.s.
****
****
E4 - Ctrl
E4 - LXR
TE4 - Ctrl
TE4 - LXR
H
NfL in plasma, pg/ml
p<0.0001
R2=0.3818
Hippocampal volume, mm3
NfL in plasma, pg/ml
p<0.0001
R2=0.3664
Cortical volume, mm3
NfL in plasma, pg/ml
p<0.0001
R2=0.2514
Ventricular volume, mm3
I
Control AIN-76 diet
7 months:
Behavioral analysis
7.5 months:
Neurodegeneration
Tau pathology
Neuroiflammation
Lipidomics
6 months old ApoE4
and P301S/ApoE4 (TE4) mice
AIN-76 diet with 10mg/kg GW3965
J
Relative Abca1/Gapdh expression
*
Control
GW3965

Fig.S5

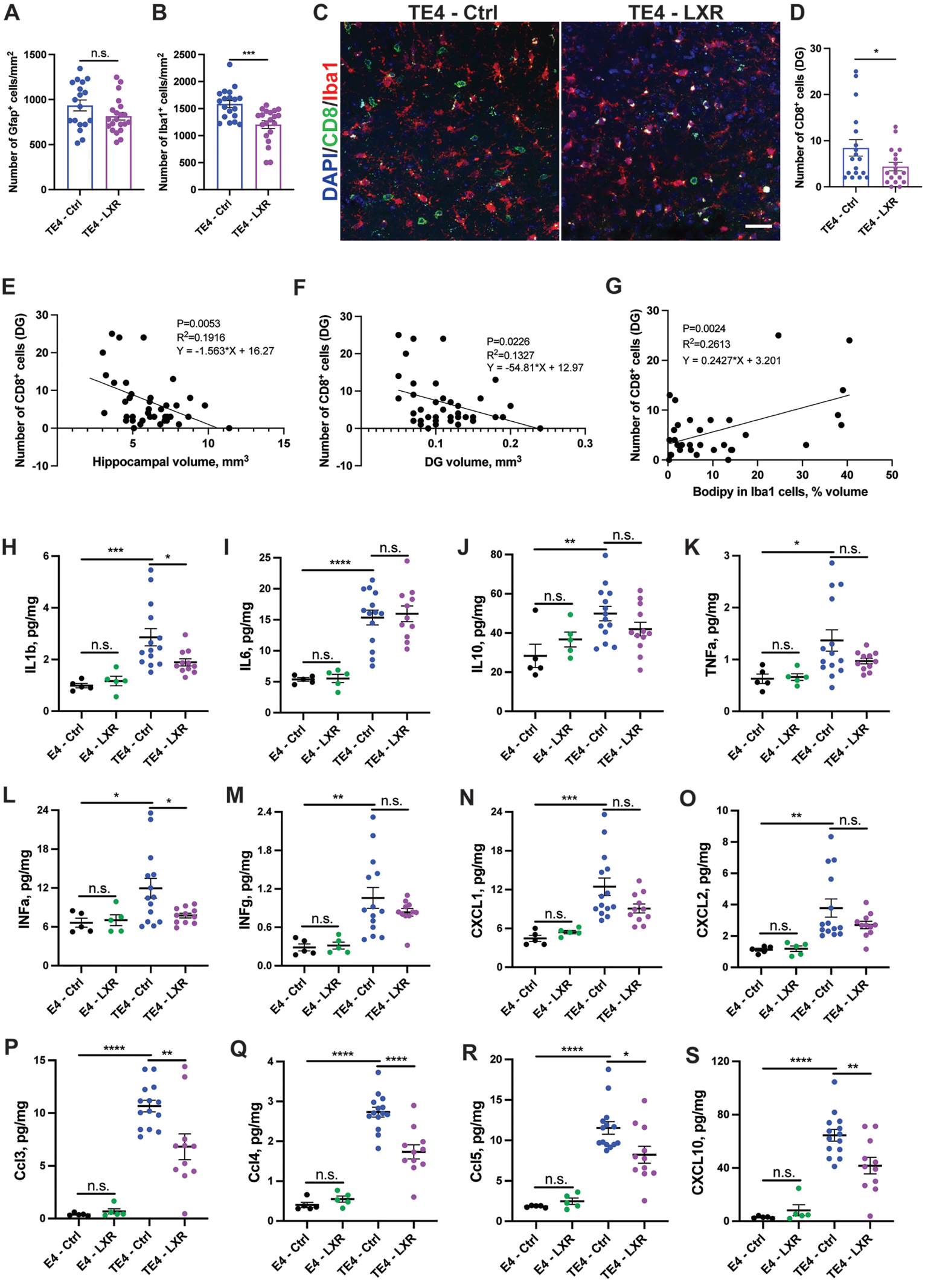
A
Number of Gfap+ cells/mm2
n.s.
TE4 - Ctrl
TE4 - LXR
B
Number of Iba1+ cells/mm2
***
C
TE4 - Ctrl
TE4 - LXR
DAPI/CD8/Iba1
D
Number of CD8+ cells (DG)
*
E
Number of CD8+ cells (DG)
P=0.0053
R2=0.1916
Y = -1.563*X + 16.27
Hippocampal volume, mm3
F
Number of CD8+ cells (DG)
P=0.0226
R2=0.1327
Y = -54.81*X + 12.97
DG volume, mm3
G
Number of CD8+ cells (DG)
P=0.0024
R2=0.2613
Y = 0.2427*X + 3.201
Bodipy in Iba1 cells, % volume
H
IL1b, pg/mg
I
IL6, pg/mg
J
IL10, pg/mg
K
TNFa, pg/mg
L
INFa, pg/mg
M
INFg, pg/mg
N
CXCL1, pg/mg
O
CXCL2, pg/mg
P
Ccl3, pg/mg
Q
Ccl4, pg/mg
R
Ccl5, pg/mg
S
CXCL10, pg/mg
E4 - Ctrl
E4 - LXR
TE4 - Ctrl
TE4 - LXR

Fig.S6

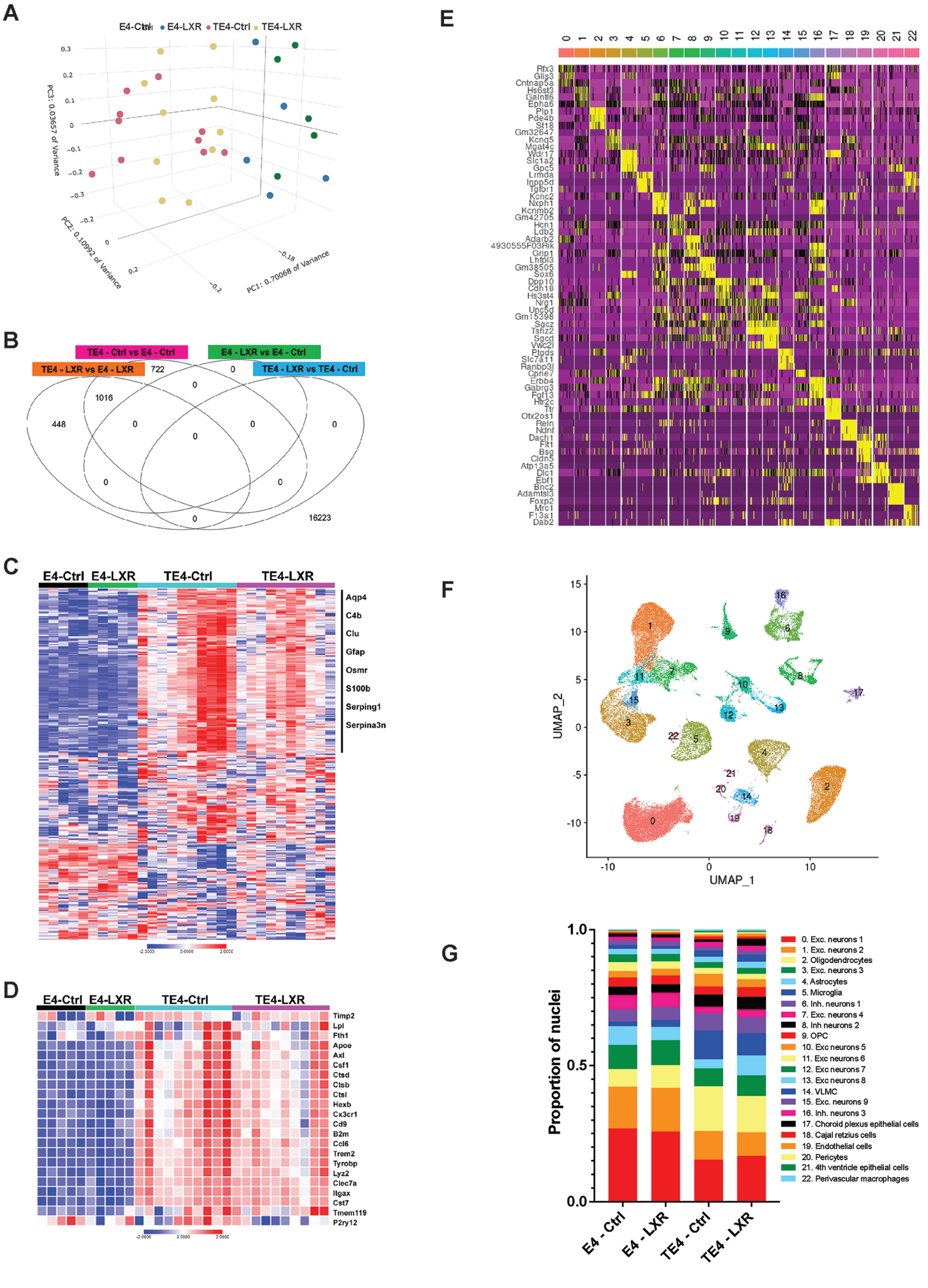
A
E4-Ctrl
E4-LXR
TE4-Ctrl
TE4-LXR
PC3: 0.03657 of Variance
PC2: 0.10992 of Variance
PC1: 0.70068 of Variance
B
TE4 - Ctrl vs E4 - Ctrl
E4 - LXR vs E4 - Ctrl
TE4 - LXR vs E4 - LXR
TE4 - LXR vs TE4 - Ctrl
722
0
1016
448
16223
C
E4-Ctrl
E4-LXR
TE4-Ctrl
TE4-LXR
Aqp4
C4b
Clu
Gfap
Osmr
S100b
Serping1
Serpina3n
D
E4-Ctrl
E4-LXR
TE4-Ctrl
TE4-LXR
Timp2
Lpl
Fth1
Apoe
Axl
Csf1
Ctsd
Ctsb
Ctsl
Hexb
Cx3cr1
Cd9
B2m
Ccl6
Trem2
Tyrobp
Lyz2
Clec7a
Itgax
Cst7
Tmem119
P2ry12
E
Rtx3
Glis3
Cntnap5a
Hs6st3
Galntl6
Epha6
Plp1
Pde4b
St18
Gm32647
Kcnq5
Mgat4c
Wdr17
Slc1a2
Gpc5
Lrmda
Inpp5d
Tgfbr1
Kcnc2
Nxph1
Kcnmb2
Gm42705
Hcn1
Ldb2
Adarb2
4930555F03Rik
Grip1
Lhfpl3
Gm38505
Sox6
Dpp10
Cdh18
Hs3st4
Nrg1
Unc5d
Gm15398
Sgcz
Tshz2
Sgcd
Vwc2l
Ptgds
Slc7a11
Ranbp3l
Cpne7
Erbb4
Gabrg3
Fgf13
Htr2c
Ttr
Otx2os1
Rein
Ndnf
Dach1
Flt1
Bsg
Cldn5
Atp13a5
Dlc1
Ebf1
Bnc2
Adamtsl3
Foxp2
Mrc1
F13a1
Dab2
F
UMAP_1
UMAP_2
G
Proportion of nuclei
E4 - Ctrl
E4 - LXR
TE4 - Ctrl
TE4 - LXR
0. Exc. neurons 1
1. Exc. neurons 2
2. Oligodendrocytes
3. Exc. neurons 3
4. Astrocytes
5. Microglia
6. Inh. neurons 1
7. Exc. neurons 4
8. Inh neurons 2
9. OPC
10. Exc neurons 5
11. Exc neurons 6
12. Exc neurons 7
13. Exc neurons 8
14. VLMC
15. Exc. neurons 9
16. Inh. neurons 3
17. Choroid plexus epithelial cells
18. Cajal retzius cells
19. Endothelial cells
20. Pericytes
21. 4th ventricle epithelial cells
22. Perivascular macrophages

Fig.S7

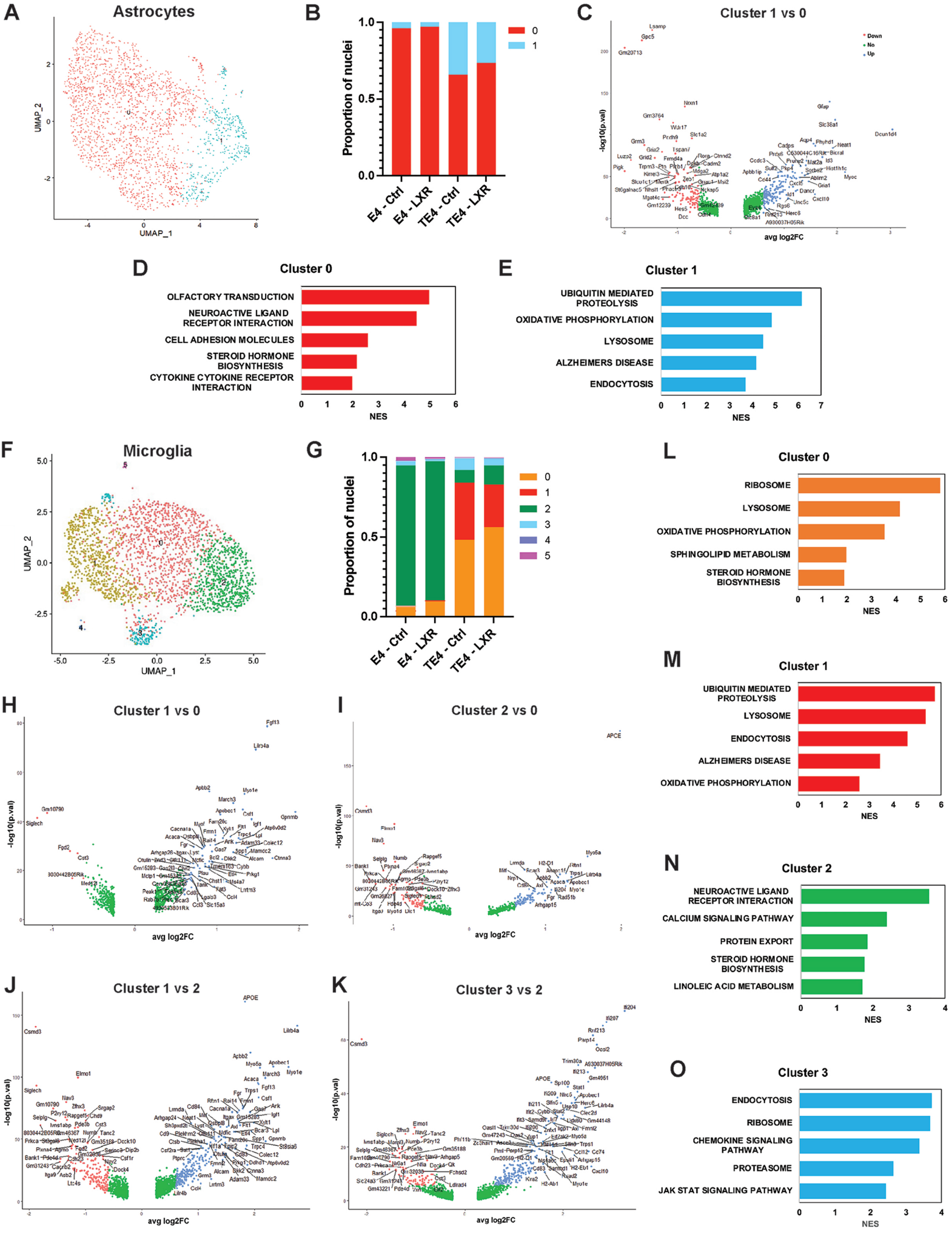
A
Astrocytes
UMAP_2
UMAP_1
B
Proportion of nuclei
0
1
E4 - Ctrl
E4 - LXR
TE4 - Ctrl
TE4 - LXR
C
Cluster 1 vs 0
Down
No
Up
-log10(p.val)
avg log2FC
D
Cluster 0
OLFACTORY TRANSDUCTION
NEUROACTIVE LIGAND RECEPTOR INTERACTION
CELL ADHESION MOLECULES
STEROID HORMONE BIOSYNTHESIS
CYTOKINE CYTOKINE RECEPTOR INTERACTION
NES
E
Cluster 1
UBIQUITIN MEDIATED PROTEOLYSIS
OXIDATIVE PHOSPHORYLATION
LYSOSOME
ALZHEIMERS DISEASE
ENDOCYTOSIS
NES
F
Microglia
UMAP_2
UMAP_1
G
Proportion of nuclei
0
1
2
3
4
5
E4 - Ctrl
E4 - LXR
TE4 - Ctrl
TE4 - LXR
L
Cluster 0
RIBOSOME
LYSOSOME
OXIDATIVE PHOSPHORYLATION
SPHINGOLIPID METABOLISM
STEROID HORMONE BIOSYNTHESIS
NES
M
Cluster 1
UBIQUITIN MEDIATED PROTEOLYSIS
LYSOSOME
ENDOCYTOSIS
ALZHEIMERS DISEASE
OXIDATIVE PHOSPHORYLATION
NES
H
Cluster 1 vs 0
-log10(p.val)
avg log2FC
I
Cluster 2 vs 0
-log10(p.val)
avg log2FC
N
Cluster 2
NEUROACTIVE LIGAND RECEPTOR INTERACTION
CALCIUM SIGNALING PATHWAY
PROTEIN EXPORT
STEROID HORMONE BIOSYNTHESIS
LINOLEIC ACID METABOLISM
NES
J
Cluster 1 vs 2
-log10(p.val)
avg log2FC
K
Cluster 3 vs 2
-log10(p.val)
avg log2FC
O
Cluster 3
ENDOCYTOSIS
RIBOSOME
CHEMOKINE SIGNALING PATHWAY
PROTEASOME
JAK STAT SIGNALING PATHWAY
NES

Fig.S8

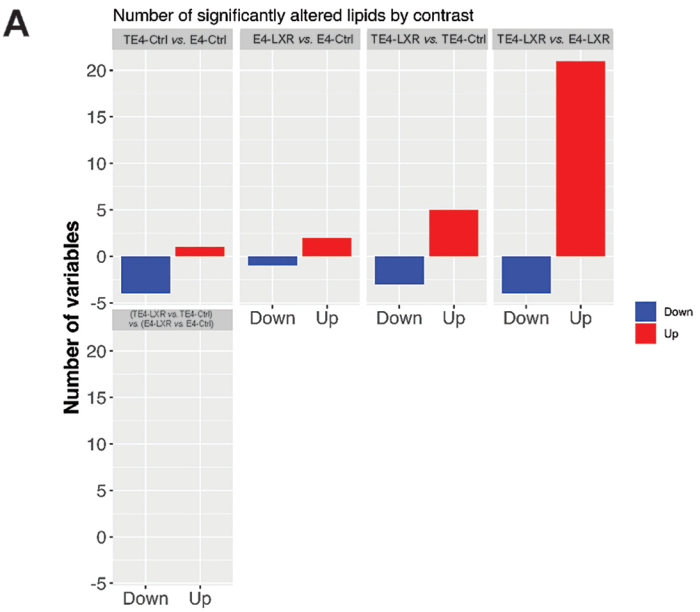
A
Number of significantly altered lipids by contrast
TE4-Ctrl vs. E4-Ctrl
E4-LXR vs. E4-Ctrl
TE4-LXR vs. TE4-Ctrl
TE4-LXR vs. E4-LXR
(TE4-LXR vs TE4-Ctrl) vs (E4-LXR vs E4-Ctrl)
Number of variables
Down
Up

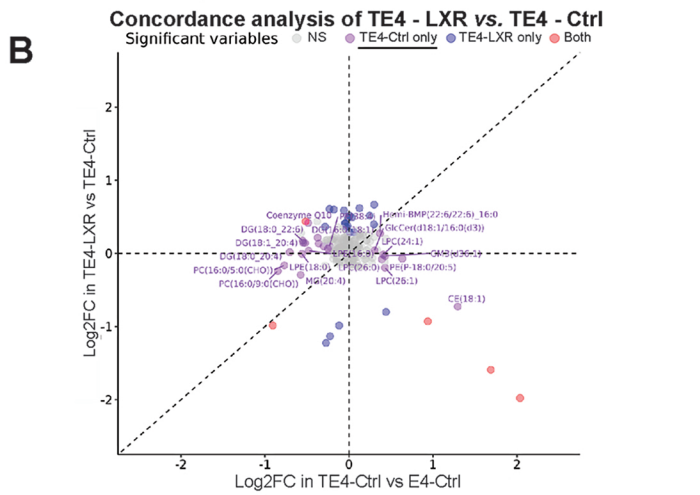
B
Concordance analysis of TE4 - LXR vs. TE4 - Ctrl
Significant variables NS TE4-Ctrl only TE4-LXR only Both
Log2FC in TE4-LXR vs TE4-Ctrl
Log2FC in TE4-Ctrl vs E4-Ctrl

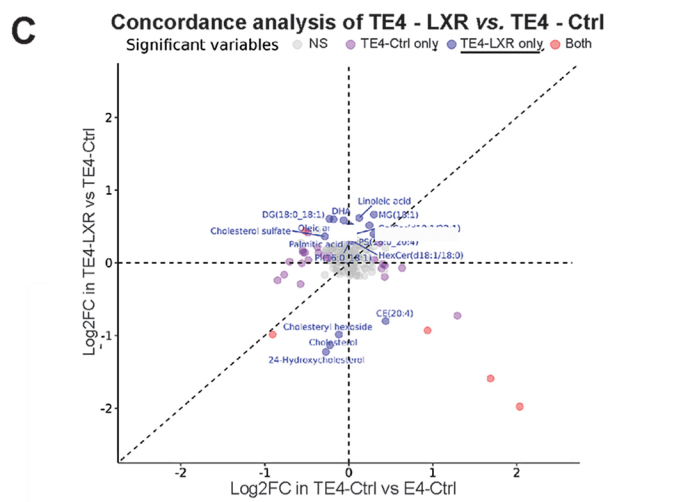
C
Concordance analysis of TE4 - LXR vs. TE4 - Ctrl
Significant variables NS TE4-Ctrl only TE4-LXR only Both
Log2FC in TE4-LXR vs TE4-Ctrl
Log2FC in TE4-Ctrl vs E4-Ctrl

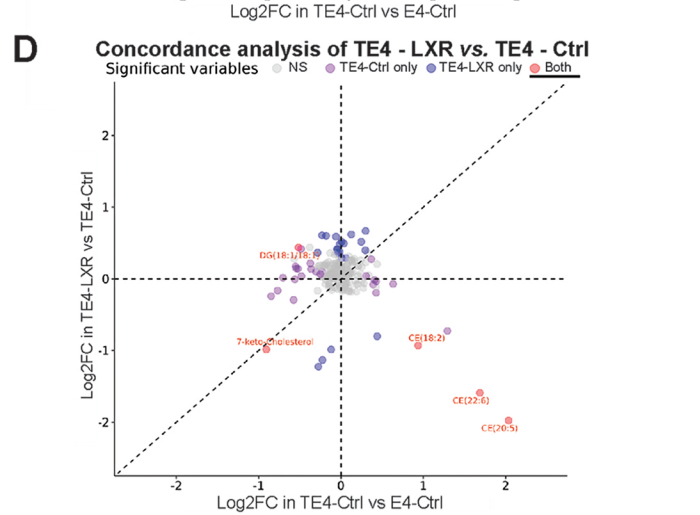
D
Concordance analysis of TE4 - LXR vs. TE4 - Ctrl
Significant variables NS TE4-Ctrl only TE4-LXR only Both
Log2FC in TE4-LXR vs TE4-Ctrl
Log2FC in TE4-Ctrl vs E4-Ctrl

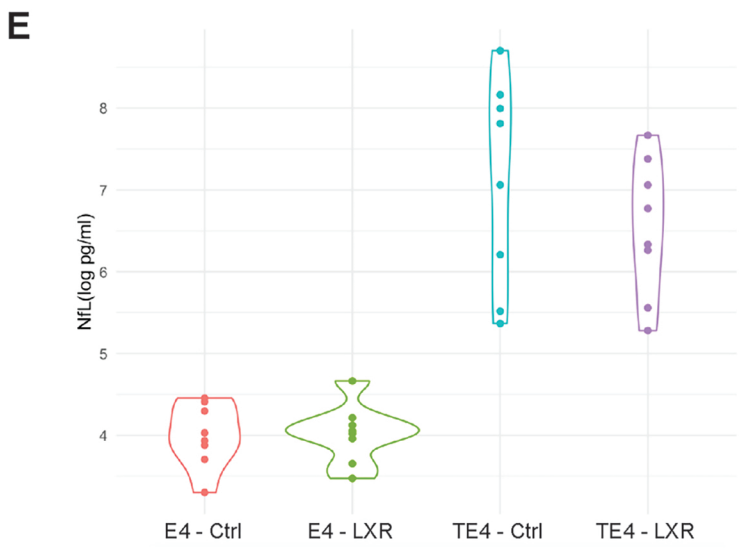
E
NfL(log pg/ml)
E4 - Ctrl
E4 - LXR
TE4 - Ctrl
TE4 - LXR

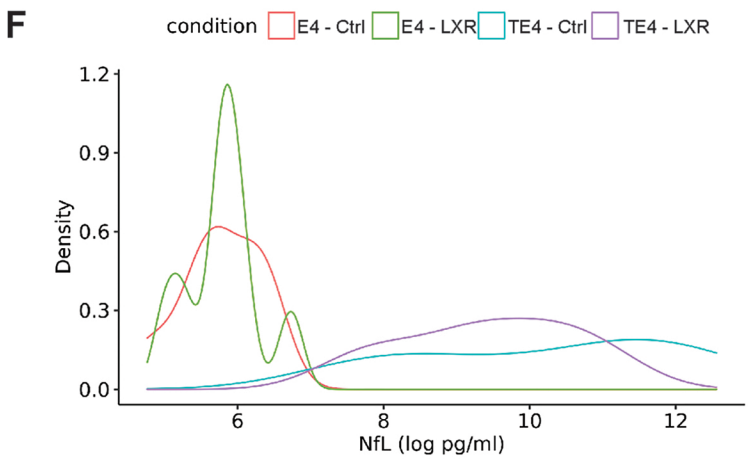
F
condition E4 - Ctrl E4 - LXR TE4 - Ctrl TE4 - LXR
Density
NfL (log pg/ml)

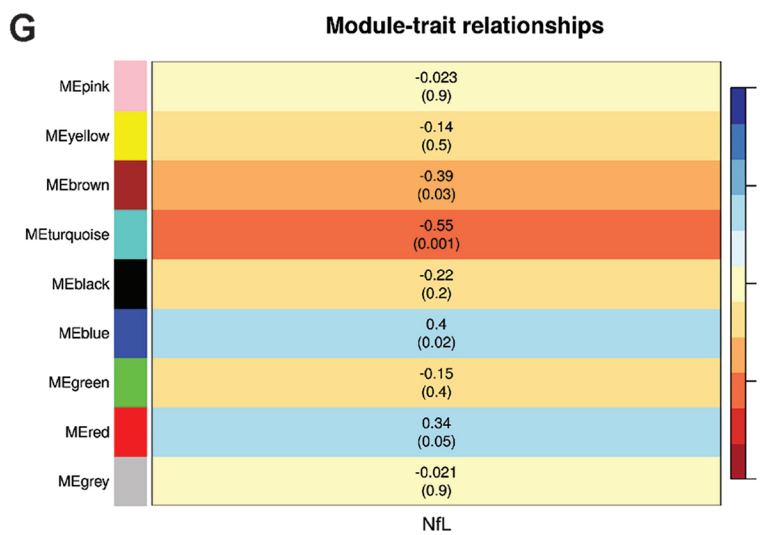
G
Module-trait relationships
MEpink -0.023 (0.9)
MEyellow -0.14 (0.5)
MEbrown -0.39 (0.03)
MEturquoise -0.55 (0.001)
MEblack -0.22 (0.2)
MEblue 0.4 (0.02)
MEgreen -0.15 (0.4)
MEred 0.34 (0.05)
MEgrey -0.021 (0.9)
NfL

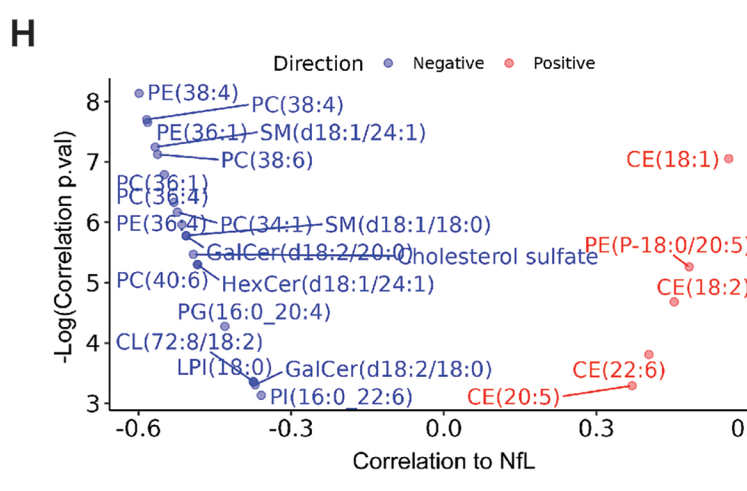
H
Direction Negative Positive
-Log(Correlation p.val)
Correlation to NfL

Fig.S9

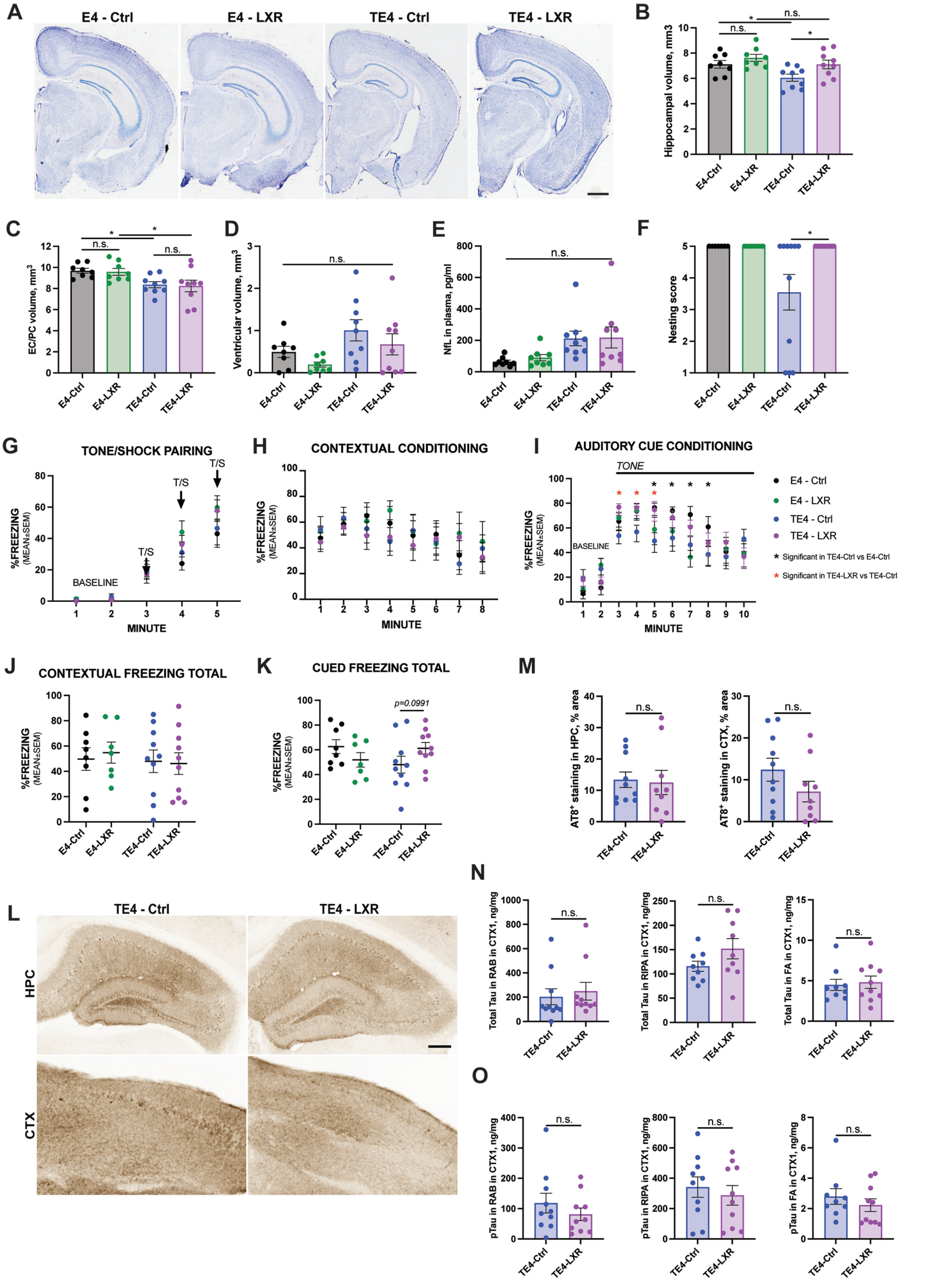
A
E4 - Ctrl
E4 - LXR
TE4 - Ctrl
TE4 - LXR
B
Hippocampal volume, mm3
n.s.
C
EC/PC volume, mm3
D
Ventricular volume, mm3
E
NfL in plasma, pg/ml
F
Nesting score
G
TONE/SHOCK PAIRING
%FREEZING (MEAN±SEM)
BASELINE
T/S
MINUTE
H
CONTEXTUAL CONDITIONING
I
AUDITORY CUE CONDITIONING
TONE
Significant in TE4-Ctrl vs E4-Ctrl
Significant in TE4-LXR vs TE4-Ctrl
J
CONTEXTUAL FREEZING TOTAL
K
CUED FREEZING TOTAL
p=0.0991
M
AT8+ staining in HPC, % area
AT8+ staining in CTX, % area
N
Total Tau in RAB in CTX1, ng/mg
Total Tau in RIPA in CTX1, ng/mg
Total Tau in FA in CTX1, ng/mg
L
HPC
CTX
O
pTau in RAB in CTX1, ng/mg
pTau in RIPA in CTX1, ng/mg
pTau in FA in CTX1, ng/mg

Fig.S10

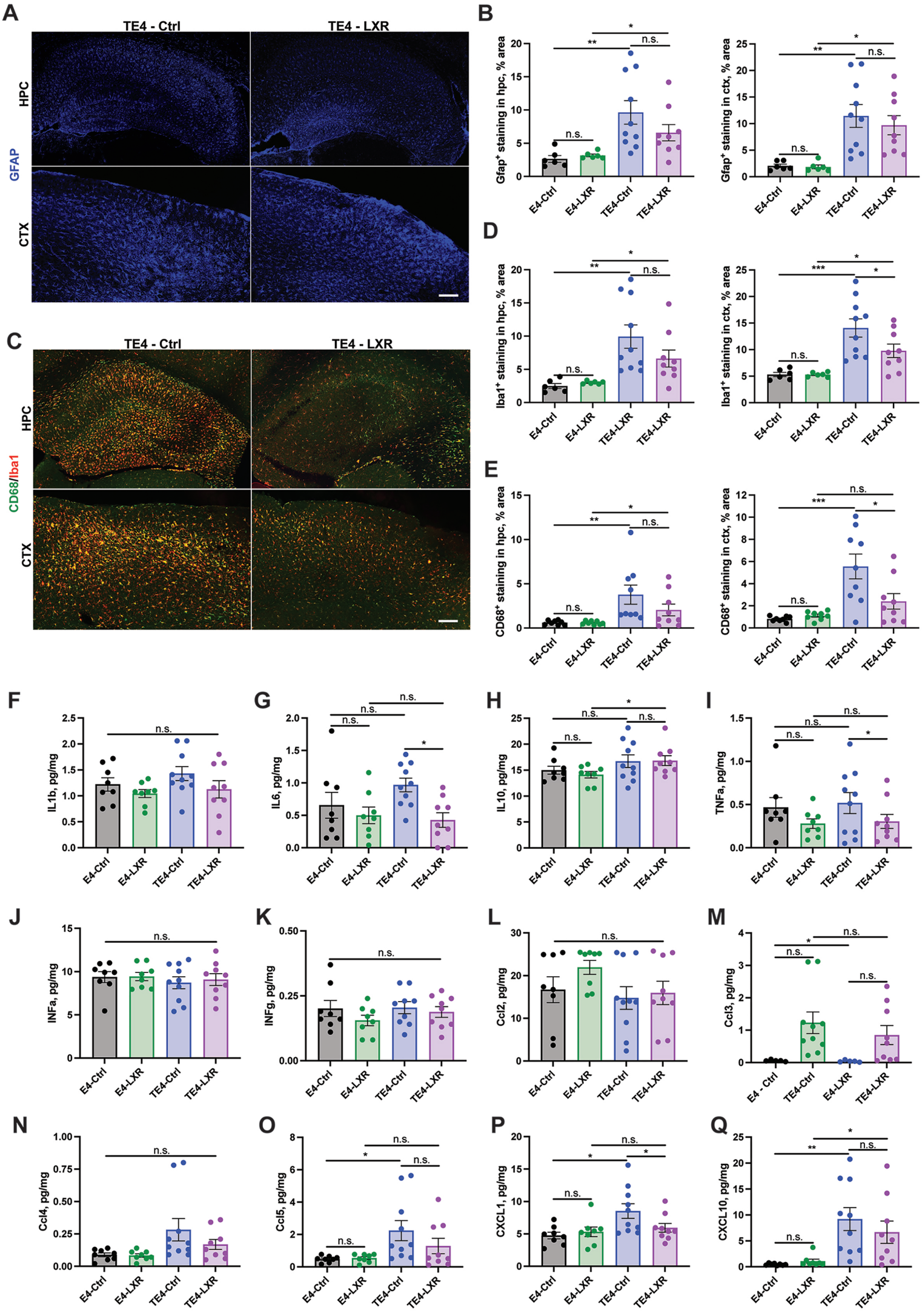
A
TE4 - Ctrl
TE4 - LXR
HPC
CTX
GFAP
B
Gfap+ staining in hpc, % area
Gfap+ staining in ctx, % area
C
TE4 - Ctrl
TE4 - LXR
HPC
CTX
CD68/Iba1
D
Iba1+ staining in hpc, % area
Iba1+ staining in ctx, % area
E
CD68+ staining in hpc, % area
CD68+ staining in ctx, % area
F
IL1b, pg/mg
G
IL6, pg/mg
H
IL10, pg/mg
I
TNFa, pg/mg
J
INFa, pg/mg
K
INFg, pg/mg
L
Ccl2, pg/mg
M
Ccl3, pg/mg
N
Ccl4, pg/mg
O
Ccl5, pg/mg
P
CXCL1, pg/mg
Q
CXCL10, pg/mg
E4-Ctrl
E4-LXR
TE4-Ctrl
TE4-LXR
E4 - Ctrl
n.s.

Fig.S11

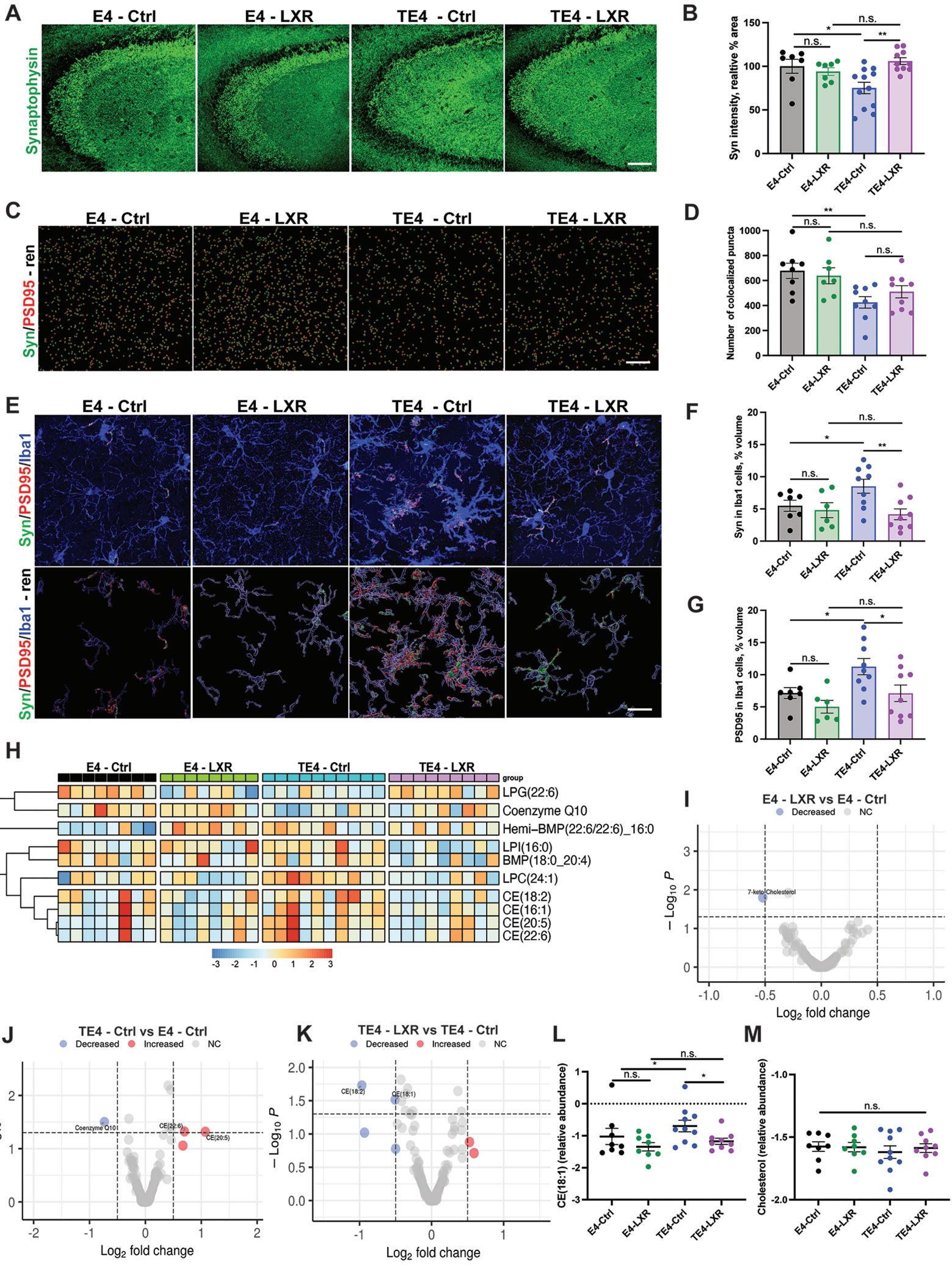
A
E4 - Ctrl
E4 - LXR
TE4 - Ctrl
TE4 - LXR
Synaptophysin
B
Syn intensity, realtive % area
n.s.
*
**
E4-Ctrl
E4-LXR
TE4-Ctrl
TE4-LXR
C
Syn/PSD95 - ren
D
Number of colocalized puncta
E
Syn/PSD95/Iba1
Syn/PSD95/Iba1 - ren
F
Syn in Iba1 cells, % volume
G
PSD95 in Iba1 cells, % volume
H
group
LPG(22:6)
Coenzyme Q10
Hemi–BMP(22:6/22:6)_16:0
LPI(16:0)
BMP(18:0_20:4)
LPC(24:1)
CE(18:2)
CE(16:1)
CE(20:5)
CE(22:6)
I
E4 - LXR vs E4 - Ctrl
Decreased
NC
7-keto Cholesterol
– Log10 P
Log2 fold change
J
TE4 - Ctrl vs E4 - Ctrl
Increased
Coenzyme Q10
CE(22:6)
CE(20:5)
K
TE4 - LXR vs TE4 - Ctrl
CE(18:2)
CE(18:1)
L
CE(18:1) (relative abundance)
M
Cholesterol (relative abundance)

Fig.S12

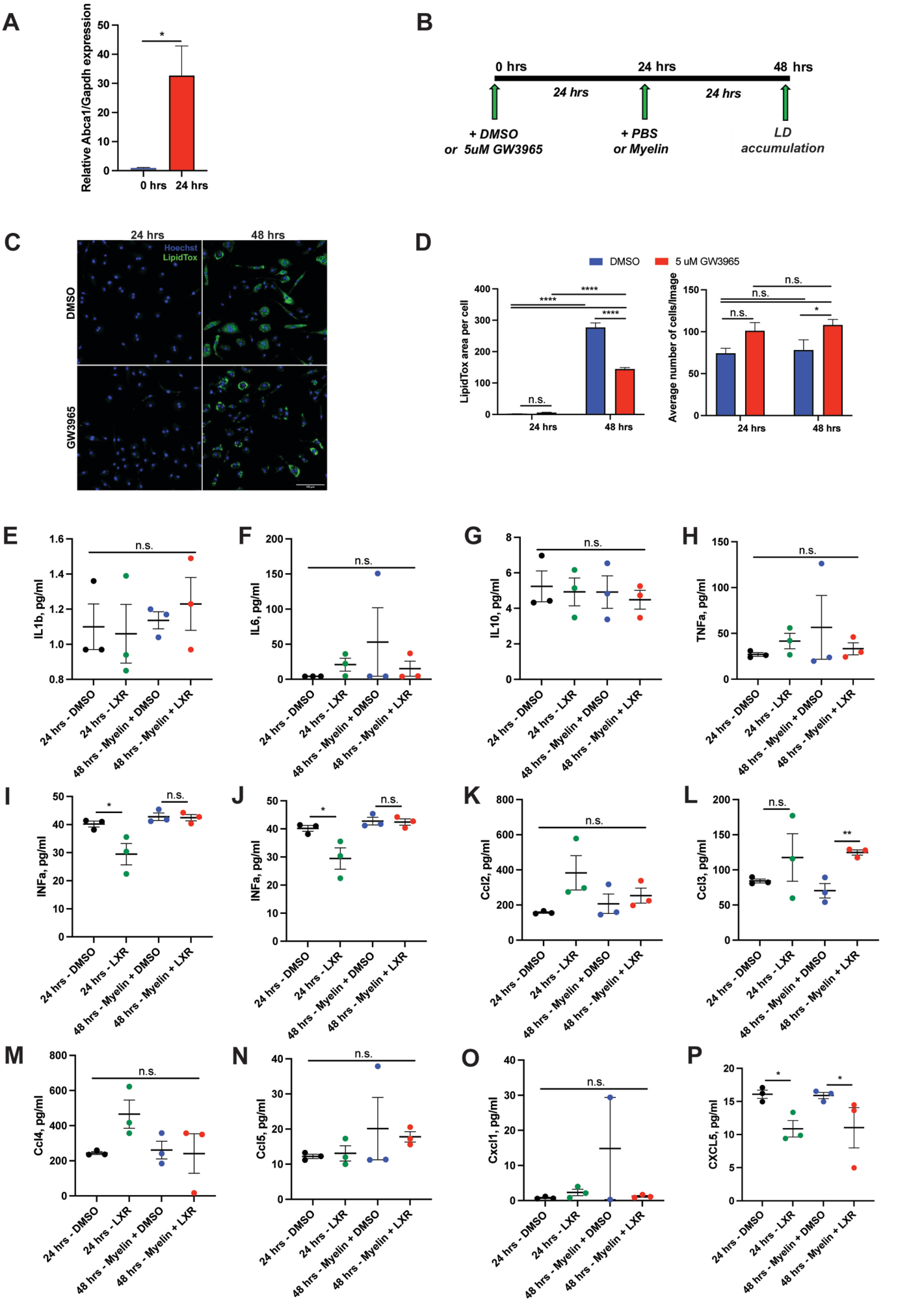
A
Relative Abca1/Gapdh expression
0 hrs
24 hrs
B
0 hrs
24 hrs
48 hrs
24 hrs
24 hrs
+ DMSO
or 5uM GW3965
+ PBS
or Myelin
LD
accumulation
C
24 hrs
48 hrs
Hoechst
LipidTox
DMSO
GW3965
D
DMSO
5 uM GW3965
LipidTox area per cell
Average number of cells/Image
n.s.
E
IL1b, pg/ml
F
IL6, pg/ml
G
IL10, pg/ml
H
TNFa, pg/ml
I
INFa, pg/ml
J
INFa, pg/ml
K
Ccl2, pg/ml
L
Ccl3, pg/ml
M
Ccl4, pg/ml
N
Ccl5, pg/ml
O
Cxcl1, pg/ml
P
CXCL5, pg/ml
24 hrs - DMSO
24 hrs - LXR
48 hrs - Myelin + DMSO
48 hrs - Myelin + LXR

Fig.S1. Related to Fig.1 and 2. Forebrain lipidomic analysis in 9.5-month-old mice. **(**A) Schematic diagram of lipidomics/FACS-coupled with lipidomics experiment. (B) Number of significantly altered lipids detected in E3 *vs.* EKO; E4 *vs.* EKO; E4 *vs.* E3; TEKO *vs.* EKO; TE3 *vs.* E3; TE4 *vs.* E4; ((TE4 *vs.* E4) vs (TE KO *vs.* EKO)); ((TE3 *vs.* E3) vs (TEKO *vs.* EKO)); ((TE4 *vs.* E4) vs (TE3 *vs.* E3)) mice. (C) Volcano plot of differentially abundant lipids in E3 *vs.* EKO mice. (D) Volcano plot of differentially abundant lipids in E4 *vs.* EKO mice. (E-F) Concordance analysis of differentially abundant lipids in (E4 *vs.* EKO) *vs.* (E3 *vs.* EKO). (G) Volcano plot of differentially abundant lipids in TE3 *vs.* E3 mice. (H) Volcano plot of differentially abundant lipids in TEKO *vs.* EKO mice. (I) Volcano plot of differentially abundant lipids in TE3 *vs.* TEKO mice. (J) Volcano plot of differentially abundant lipids in TE4 *vs.* TE3 mice. N=12 (6M and 6F)/genotype. $p<0.05$. Log2FC>0.5. 181 variables detected.

Fig.S2. Related to Fig.1 and 2. Lipidomic analysis in forebrain tissues and in FACS-isolated astrocytes and microglia in 9.5-month-old mice. (A-B) Concordance analysis of differentially abundant lipids in (TE3 *vs.* E3) vs (TEKO *vs.* EKO). (C-E) Concordance analysis of differentially abundant lipids in (TE4 *vs.* E4) vs (TEKO *vs.* EKO). (F) Heatmap of significantly changed lipids in FACS-isolated astrocytes from 9.5-month-old EKO and TEKO, E3 and TE3, E4 and TE4 mice. (G) Heatmap of significantly changed lipids in FACS-isolated astrocytes from 9.5-month-old EKO and TEKO, E3 and TE3, E4 and TE4 mice. N=12 (6M and 6F)/genotype. $p<0.05$. Log2FC>0.5. 181 variables detected. R square test in C-E.

Fig.S3. Related to Fig.2. E06-positive oxidized lipid accumulation in 9.5-month-old mice. (A) Representative E06 (green), Iba1 (red) and GFAP (blue) co-immunostaining in hippocampus of 9.5-month-old mice. (B) Quantification of E06 signal within GFAP-positive astrocytes. (C) Quantification of E06 signal within Iba1-positive microglia. (D) Correlation between the level of BODIPY staining in Iba1-positive microglia and hippocampal (left), piriform/entorhinal cortex (middle), and ventricular (right) volumes. (E) Correlation between the level of E06 staining in GFAP-positive astrocytes and hippocampal (left), piriform/entorhinal cortex (middle), and left ventricle (right) volumes.

(F) Correlation between the level of E06 staining in Iba1-positive microglia and hippocampal (left), piriform/entorhinal cortex (middle), and left ventricle (right) volumes. *p<0.05; ** p<0.01; N.S. – non-significant. One-way ANOVA in B-C. R square test in D-F.

Fig.S4. Related to Fig.3. LXR agonist GW3965 treatment in 9.5 and 7.5 month old P301S/ApoE4 (TE4) mice. (A) Schematic diagram of treatment of ApoE4 (E4) and P301S/ApoE4 (TE4) mice with LXR agonist GW3965 from 6 to 9.5 months. (B) Relative Abca1, Abcg1, Abca7 and hAPOE mRNA expression in hippocampus of 9.5-month-old ApoE4 mice treated from 6 to 9.5 months with control or GW3965 (LXR) diets. (C-D) Abca1 protein levels (C) with quantification (D) in 9.5-month-old mice. (E) Representative Cresyl Violet staining of dentate gyrus (DG) neurons. (F-G) Quantification of DG neuronal layer volume (F) and thickness (G). (H) Correlation of NfL levels in plasma with hippocampal (left), cortical (middle), and ventricular (right) brain volumes. (I) Schematic diagram of treatment of ApoE4 (E4) and P301S/ApoE4 (TE4) mice with LXR agonist GW3965 from 6-7.5 months. (J) Relative Abca1 mRNA expression in hippocampus of 7.5 months old ApoE4 mice treated from 6 to 7.5 month with control or GW3965 (LXR) diets. Male mice. Scale Bar in E: 50uM. *p<0.05; **** p<0.0001; N.S. – non-significant. Student's T-Test in B, D, J. One-Way ANOVA in F and G. R square test in H.

Fig. S5. Related to Fig.4. LXR agonist GW3965 treatment reduces T cells numbers and cytokine/chemokine levels in 9.5-month-old TE4. (A) Number of $Gfap^+$ cells in hippocampus of 9.5-month-old TE4 mice on Ctrl vs LXR diet. (B) Number of $Iba1^+$ cells in hippocampus of 9.5-month-old TE4 mice on Ctrl vs LXR diet. (C) Representative CD8 (green) and Iba1 (red) co-immunostaining with DAPI in dentate gyrus (DG) of 9.5-month-old TE4 mice. (D) Quantification of number of DAPI and CD8-positive/Iba1-negative T cells in (A). (E-G) Correlation of number of CD8-positive T cells with hippocampal (E), DG volumes (F), and level of BODIPY staining in hippocampal microglia (G). (H-S) Levels of cytokines/chemokines in hippocampus of 9.5-month-old mice. Each dot represents one animal: N (E4 – Ctrl) = 15; N (E4 – LXR) = 15; N (TE4 - Ctrl) = 18; N (TE4-LXR) =21.

Male mice. Scale bar in A: 50 um. *p<0.05; ** p<0.01; *** p<0.001. N.S. – non-significant. Student`s T-test in A-B, D. R square test in E-G. One-way ANOVA in H-S.

Fig.S6. Related to Fig.6. Bulk and snRNAseq analysis in 9.5-month-old TE4 mice. (A) PCA analysis of gene expression changes in ApoE4 and P301S/ApoE4 (TE4) *vs.* ApoE4 (E4) mice treated with control (Ctrl) or GW3965 (LXR) diet from 6 to 9.5 months. P.adj. <0.05. N(E4/treatment) =5; N(TE4/treatment) =10. Male mice. (B) Venn Diagram representing number of DEGs identified with P.adj. <0.05. (C) Heatmap for disease-associated astrocyte genes (DAA). (D) Heatmap for disease-associated microglia genes (DAM). (E) Heatmap demonstrating the expression of cell-type specific markers across 23 cell types identified by snRNAseq in 9.5-month-old E4 and TE4) mice treated with either control (Ctrl) or 10mg/kg GW3965 LXR agonist diet (LXR). (F) UMAP of 23 cell types identified by snRNAseq. (G) Proportion of 23 different cell populations by genotype/treatment. P.adj. <0.05.

Fig.S7. Related to Fig.6. Gene expression in astrocytes and microglia from snRNAseq analysis in 9.5-month-old TE4 mice. (A) UMAP of 2 astrocyte clusters identified by snRNAseq in 9.5-month-old ApoE4 and P301S/ApoE4 (TE4) mice treated with either control (Ctrl) or 10mg/kg GW3965 LXR agonist diet (LXR). (B) Proportion of 2 astrocyte clusters by genotype/treatment. (C) Volcano plot comparing DEGs between clusters 0 and 1. (D) Top 5 biological pathways (KEGG) enriched in Cluster 0. (E) Top 5 biological pathways (KEGG) enriched in Cluster 1. (F) UMAP of 6 microglial clusters identified by snRNAseq in 9.5-month-old ApoE4 and P301S/ApoE4 (TE4) mice treated with either control (Ctrl) or 10mg/kg GW3965 LXR agonist diet (LXR). (G) Proportion of 6 microglia clusters by genotype/treatment. (H) Volcano plot comparing DEGs between clusters 1 and 0. (I) Volcano plot comparing DEGs between clusters 2 and 0. (J) Volcano plot comparing DEGs between clusters 1 and 2. (K) Volcano plot comparing DEGs between clusters 3 and 2. (L) Top 5 biological pathways (KEGG) enriched in Cluster 0. (L) Top 5 biological pathways (KEGG) enriched in Cluster 1. (M) Top 5 biological pathways (KEGG) enriched in Cluster 2. (N) Top 5 biological pathways (KEGG) enriched in Cluster 3.

Fig.S8. Related to Fig.7. Lipidomic analysis in 9.5-month-old TE4 mice treated with an LXR agonist GW3965. (A) Number of significantly altered lipids detected in TE4-Ctrl *vs.* E4-Ctrl; E4-LXR *vs.* E4-Ctrl; TE4-LXR *vs.* TE4-Ctrl; TE4-LXR v *vs.* E4-LXR; ((TE4-LXR *vs.* E4-LXR) *vs.* (TE4-Ctrl *vs.* E4-Ctrl)) mice. (B-D) Concordance analysis of differentially abundant lipids in (TE4-LXR *vs.* TE4-Ctrl) *vs.* (TE4-Ctrl *vs.* E4-Ctrl). (E) NfL levels in plasma of 9.5-month-old ApoE4 and TE4 mice on control *vs.* LXR diets used for lipidomics analysis. N=8/group. Male mice. (F) Correlation between lipid levels in forebrain and NfL levels in plasma of 9.5-month-old mice. (G) WLCNA modules of brain lipid to NfL plasma correlations. Turquoise module shows strong correlation with NfL levels in plasma. R value – top, P-value in brackets. (H) Correlation analysis between lipid abundance in brain and NfL levels in plasma. P.adj. <0.05.

Fig. S9. Related to Fig.3. LXR agonist GW3965 treatment reduces neurodegeneration, improves behavior and reduces phospho-Tau levels in 7.5 month old TE4 mice. (A) Representative Cresyl Violet staining of brain sections from 7.5 month old E4 and TE4 mice treated with either control (Ctrl) or 10mg/kg GW3965 LXR agonist diet (LXR) from 6 to 7.5 months. (B-D) Quantification of hippocampal (B), entorhinal/piriform (EC/PC) cortical (C) and ventricular volumes in 7.5 month old mice (D). (E) Neurofilament light chain (NfL) levels in plasma of 7.5 month old mice. (F) Nesting behavior score in 7.5 months old mice. 0 – no nestlets used. 1 - <10% nestlets used. 2 – 20-50% nestlets used. 3 – 50-90% nestlets used. 4 - <10% nestlets unused. 5 – 100% nestlets used. (G-K) Fear Conditioning in 7-7.5 month old mice: Tone/Shock pairing (G); Contextual Conditioning over 8 min and Total Contextual Freezing (H and J); Auditory Cued Conditioning over 10 min and Total Cued Freezing (I and K). (L) Representative immunohistochemical staining of AT8 phospho-tau in hippocampus (hpc) and cortex (ctx) of 7.5 month old mice. (M) Quantification of AT8 signal in hippocampus and cortex. (N)

Total tau levels in cortical RAB, RIPA and FA fractions. (O) Phospho-tau (AT8) levels in cortical RAB, RIPA and FA fractions. Each dot represents one animal: N (E4 – Ctrl) = 7; N (E4 – LXR) = 7; N (TE4 - Ctrl) = 11; N (TE4-LXR) =9. Male mice. Scale Bar in A: 1 mm; L: 100 um. *p<0.05; N.S. – non-significant. One-way ANOVA in B-E. Chi-square test in F. Two-way ANOVA in J-K. Significant genotype-treatment interaction with p=0.0119 in (K). Student's T-Test in M-O.

Fig. S10. Related to Fig.4. LXR agonist GW3965 treatment reduces microglial activation and cytokine/chemokine levels in 7.5 month old TE4. (A) Representative GFAP immunostaining in hippocampus (hpc) and cortex (ctx) of 9.5-month-old E4 and TE4 mice treated with either control (Ctrl) or 10mg/kg GW3965 LXR agonist diet (LXR) from 6 to 7.5 months. (B) Quantification of (A). (C) Representative CD68 (green) and Iba1 (red) co-immunostaining in hippocampus (hpc) and cortex (ctx). (D-E) Quantification of Iba1 (D) and CD68 staining in (C). (F-Q) Levels of cytokines/chemokines in hippocampus of 7.5 month old mice. Each dot represents one animal: N (E4 – Ctrl) = 7; N (E4 – LXR) = 7; N (TE4 - Ctrl) = 11; N (TE4-LXR) =9. Male mice. Scale bar in A: 100 um. Male mice. Scale bar in A and C: 100 um. *p<0.05; ** p<0.01; *** p<0.001. N.S. – non-significant. One-way ANOVA.

Fig. S11. Related to Fig.5. LXR agonist GW3965 treatment reduces synaptic loss and forebrain lipid accumulation in 7.5 month old TE4 mice. (A and B) Representative synaptophysin immunostaining in CA3 area of hippocampus from 7.5 month old E4 and TE4 mice treated with either control (Ctrl) or 10mg/kg GW3965 LXR agonist diet (LXR) from 6 to 7.5 months and its quantification (B). (C-D) Representative 3D-rendering of co-localized synaptophysin (Syn) and PSD95 puncta in CA3 area of hippocampus and quantification of co-localized puncta in (D). (E) Representative synaptophysin (Syn, green) and PSD95 (red) inside Iba1-postive microglia (blue) from 7.5 old mice with 3D-rendering. (F-G) Quantification of synaptophysin (Syn) (F) and PSD95 (G) volumes within Iba1-positive microglia. (H) Heatmap of significantly changed lipids in forebrains of 7.5

month old E4 or TE4 mice. (I) Volcano plot of differentially abundant lipids in E4-LXR *vs.* E4-Ctrl mice. (J) Volcano plot of differentially abundant lipids in TE4-LXR *vs.* E4-LXR mice. (K) Volcano plot of differentially abundant lipids in TE4-LXR *vs.* TE4-Ctrl mice. (L) Relative levels of CE (18:1) in forebrains of 7.5 old mice. (M) Relative levels of free cholesterol in forebrains of 7.5 old mice. Each dot represents one animal: N (E4 – Ctrl) = 7; N (E4 – LXR) = 7; N (TE4 - Ctrl) = 11; N (TE4-LXR) =9. Male mice. Scale bar in A: 100 um; C: 5 um; E: 10um. *p<0.05; ** p<0.01; N.S. – non-significant. One-way ANOVA in B-G, M-N. P.adj. generated by R Statistical package for all lipids detected in lipidomic profiling analysis in H-L.

Fig.S12. Related to Fig.8. LXR agonist GW3965 decreases lipid droplet accumulation in primary E4 microglia. (A) Relative Abca1 mRNA expression in primary E4 microglia treated with 5uM GW3965 or DMSO for 24 hrs. (B) Schematic diagram of myelin uptake experiment. (C) Representative images of LipidTox-positive lipid droplets in E4 microglia pre-treated with DMSO/GW3965 and exposed to myelin for 0 or 24 hrs (timepoints 24 and 48 hrs in myelin uptake). (D) LipidTox area per cell (left) and average number of cells per image analyzed (right) (timepoints 24 and 48 hrs in myelin uptake). (E-P) Levels of cytokines/chemokines in conditioned media from E4 microglia pre-treated with DMSO/GW3965 and exposed to myelin for 0 or 24 hrs (myelin uptake). *p<0.05; ** p<0.01; *** p<0.001; **** p<0.0001. N.S. – non-significant. (A) Student's t-test in A and E-P. Two-way ANOVA in D.